Milli-fluidic setup for continuous flow synthesis of organic semiconductor nanoparticles

Gwenael Bonfante, Fumiyasu Awai, Takaya Kubo, Hiroshi Segawa, Soo Hyeon Kim, Anthony Genot, Sylvain Chambon

Milli-fluidic setup for continuous flow synthesis of organic semiconductor nanoparticles

Gwenael Bonfante,[1] Fumiyasu Awai,[2] Takaya Kubo,[2] Hiroshi Segawa,[2] Soo Hyeon Kim[1] Anthony Genot[1] and Sylvain Chambon[1,3*]*

[1] LIMMS/CNRS-IIS (IRL2820), Institute of Industrial Science, The University of Tokyo, 4-6-1 Komaba, Meguro-ku, Tokyo, 153-8505, Japan

[2] RCAST, The University of Tokyo, 4-6-1 Komaba, Meguro-ku, Tokyo, 153-8904, Japan

[3] University of Bordeaux, IMS, CNRS, UMR 5218, Bordeaux INP, ENSCBP, F-33405 Talence, France

Corresponding authors: genot@iis.u-tokyo.ac.jp, sylvain.chambon@u-bordeaux.fr

Keywords: nanoprecipitation, millifluidic, organic photovoltaic, conjugated polymer, nanoparticles

Abstract

In this work, different milli-fluidic mixers were designed and fabricated for the continuous flow synthesis of organic semi-conductor nanoparticles. In particular, additive manufacturing was used, with a polyether ether ketone (PEEK) 3D printer to fabricate the mixers. Nanoprecipitation was applied to synthesis poly(3-hexylthiophene-2,5-diyl) (P3HT) nanoparticles (NP) and different mixing conditions were investigated. We show that using such setups, it is possible to control precisely the turbulences in the chip, and as a result the mixing conditions between the solvent and the anti-solvent. With such strategy, P3HT nanoparticles with 60 nm diameter were synthesized using surfactant-assisted nanoprecipitation. Composite donor:acceptor nanoparticles were also designed and the presence of PCBM in the NP lead to a further decrease of the size, down to 49 nm. This work highlights the benefits of using milli-fluid systems for large-scale and reproducible synthesis of organic semi-conductor nanoparticles.

1. Introduction

Organic semiconductors nanoparticles have been developed and studied in different application fields, from photocatalysis for hydrogen generation[1,2] to sensors and imaging,[3,4] as well as their use to fabricate organic photovoltaic (OPV) devices.[5–7] For the specific field of OPV, water-based nanoparticles dispersions are used to reduce the environmental impact of this technology.[5] Indeed, OPV devices are mostly fabricated from printed techniques (spin-coating, Dr blading, slot-die coating…) using inks based on aromatic and/or chlorinated solvents, toxic for the operators and the environment. A solution to reduce the toxicity of the process is to work with water and develop organic semiconductor colloidal inks which can be used as an intermediate to fabricate thin active layer films.

Due to the low dielectric constant of organic semiconductors, the exciton formed upon absorption of photons is still strongly bound (Frenkel exciton) and needs to be dissociated to form free charges. It is generally achieved by associating in the active layer, a donor material and an acceptor material with different energy levels to efficiently dissociate the excitons. However, since the exciton diffusion length is relatively short, from 8 to 50 nm,[8–11] sufficiently intimate morphology, called bulk-heterojunction,[12] between the two materials is necessary to allow efficient exciton dissociation. As a consequence, the donor-acceptor active layer morphology needs to be carefully controlled and thus is the nanoparticles morphology. Size and morphology are then important criteria to consider when developing NP synthesis methods.[7,13] To this aim, two main techniques have been used to generate nanoparticles: mini-emulsion and nanoprecipitation.[5] Miniemulsion technique has been the first to be applied to nanoparticle based OPV.[14,15] For a long time, the efficiencies were remaining low, mainly due to the morphology of the composite donor-acceptor nanoparticles which appeared to be core-shell when fullerene derivatives were used as acceptors.[16–18] Very recently Laval *et al.* showed that it was possible to achieve intermixed morphology by careful choice of the donor/acceptor combination to achieve low interfacial energy and PCE approaching 10% were achieved.[7] Attempts to develop single component NP (donor pure / acceptor pure) have also been done but power conversion efficiencies (PCE) of OPV devices were lower than that of composite NP, probably due to too large nanoparticles, which diameter exceeded the exciton diffusion length.[13] Nanoprecipitation works on the principle of diffusion of a good solvent in an anti-solvent – both miscible –, leading to precipitation of the polymer in solution. A solution containing the polymer to precipitate in a solvent is quickly dropped in an anti-solvent. It starts first with the formation of a suspension, followed by the nucleation of polymer nuclei and growth, ending on the agglomeration of the particles formed. Concentration of the polymeric solution and solvent/anti-solvent ratio controls mostly the size of the resulting nanoparticles. Indeed, nucleation should overrule growth and agglomeration to obtain the smallest size possible.[19,20] Nanoprecipitation technique was first successfully used in OPV with chloroform/alcohol solvent/anti-solvent systems and PCE up to 4% were achieved with P3HT:ICBA donor acceptor composite nanoparticles.[21] Later, using water as anti-solvent and surfactant assisted nanoprecipitation, devices with 7.5% efficiencies were achieved by Xie *et al.*[6] In this article, efficient removal of excess of surfactant (Pluronic F127) was achieved due to thermally sensitive critical micelle concentration (CMC). Very recently, Holmes *et al.* showed that up to 10% PCE could be achieved using surfactant-assisted nanoprecipitation with sodium dodecyl sulfate (SDS), showing that nanoprecipitation is a powerful strategy to develop water-based inks for organic photovoltaic.[22] To conclude, in the quest of developing organic semiconductor colloidal inks, either alcoholic-based or water-based, it has been shown that the size and the morphology are important parameters to control to reach high efficiency devices.[7,23]

In OPV field, the most widely used method to form nanoparticles dispersions by nanoprecipitation is the batch method. The polymeric solvent is dropped quickly in a beaker of the anti-

solvent method under strong stirring. It is a very convenient method because of its easiness of setup and the quickly observable result. However, it is a one-pot method and does not allow to screen quickly different parameters proper to nanoprecipitation such as the concentration, the ratio of solvent/ anti-solvent or the modification of the environment as the experiment is ongoing. In addition, reproducibility can be an issue in the batch method, since the mixing time between the solvent and anti-solvent is difficult to control while it is a critical parameter to control the size.[24] Micro- or milli-fluidic systems are widely utilized for the synthesis of particles by precisely controlling experimental parameters. It has been shown that using micro-fluidic chips[25,26] or millifluidic setups,[27] it is possible to finely control the mixing time and as a consequence the size of the nanoparticles.[24] Each technics has benefits and drawbacks : microfluidics allow the use of less reactant but the output is very low and chips are easy to clog; millifluidics on the other hand provide an interesting output of solution with chip easily cleanable but they require a non negligeable load of reagant. For the formation of nanoparticles in a reproducible and decent scale, millifluidics seems to be more adapted for our goal here. For example, Seaberg *et al.* were able to fabricate nanoparticles encapsulate bovine serum albumin (BSA) in a grafted poly(ethylene glycol) (PEG) shell by a millifluidic process. This process involved a laminar flow to be able to coat the BSA with a PEG layer followed by ultrasonic bath to break down the film and form the droplets. They could achieve nanoparticles ranging from 13 to 300 nm.[28] Another millifluidic system for the fabrication of drug-polysaccharide nanoparticles complex has been published by Tran *et al.* By a Y-junction and two push syringe they were able to finely tune the size of nanoparticles made of curcumin and chitosan. They were able to control the size by placing collector on different point of the output channel. They could achieve nanoparticles of 115 nm after optimizing the system.[29] Finally, several teams shown the use of millifluidic devices for the synthesis of poly (lactic co-glycolic) acid (PLGA) nanoparticles.[30–32] Indeed, PLGA is a very useful polymer in biomedical field because of its high biocompatibility. As an example, Libi *et al.* compared the synthesis of PLGA nanoparticles by batch processes and continuous flow. The ability to control the flow, the parameters of the reaction (ratio, pH, concentration of the components, etc.) are very advantageous to the continuous flow process. They could achieve size comparable between the batch process and the continuous flow: around 200 nm nanoparticles. They also showed the ability to finely tune parameters of the nanoprecipitation – such as the aqueous/ organic phase ratio or the flow rate – allowing more possibilities for formulating nanoparticles.[33] In addition, micro- or milli-fluidic setup allows flow synthesis of nanoparticles, a necessary step for upscaling the fabrication of water-based colloidal inks.

In this article, we have been developing milli-fluidic setups to precisely control the solvent/anti-solvent mixing conditions for the nanoprecipitation technique. Different kinds of milli-fluidic setups were studied, co-flow setups with a T-junction or mixing chamber using an architecture inspired by confined impinging jets setups (CIJ), allowing synthesis of 60 nm nanoparticles. The influence of different parameters, such as the flow rates and the pressure, on the nanoparticle size has been studied.

Results show that efficient control of the NP size can be done in these milli-fluidic setups and open the route for continuous synthesis of well-defined organic semiconductor nanoparticles.

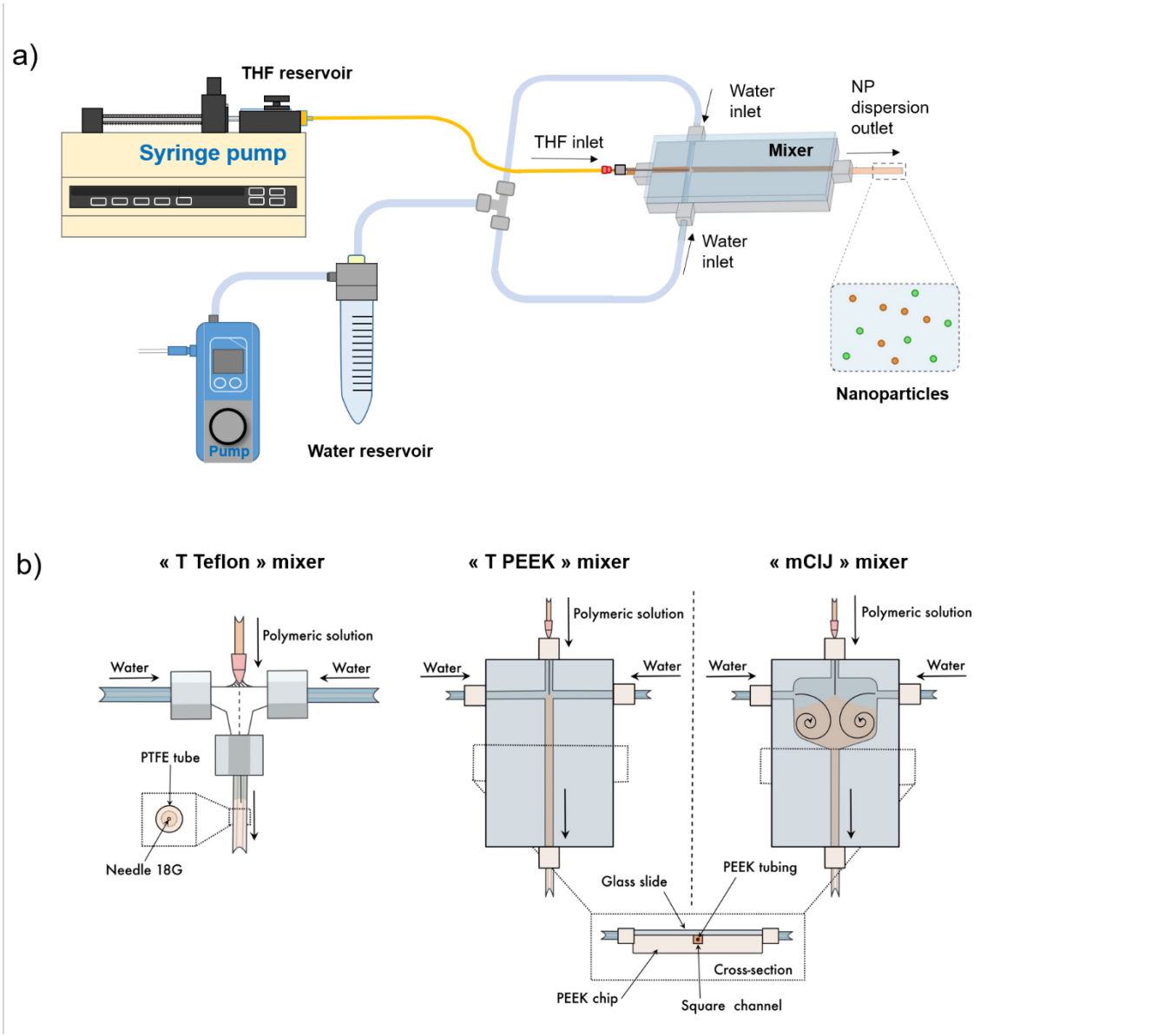

Figure 1. Schematic of a) the millifluidic setup and b) the three different milli-fluidic mixers studied referenced as: T-Teflon for a co-flow mixer made of Teflon with a circular section for water and THF inlets of 2 mm and 0.84 mm diameters respectively; T-PEEK for a co-flow mixer made of polyether ether ketone (PEEK) with a square section of 2 × 2 mm² for water inlet and circular THF inlet of 1/32" diameter; and milli confined inpinging jet (mCIJ) made of PEEK. The two mixer T-PEEK and mCIJ are differentiated by their mixing chamber: a T junction and a bigger square mixing chamber, respectively.

2. Materials and methods

Materials. The organic semiconductors poly(3-hexylthiophene-2,5-diyl) (P3HT) and [6,6]-Phenyl C61 butyric acid methyl ester (PCBM) were provided by Solaris Chem. (Canada). The tetrahydrofuran

(stabilized by BHT) was provided by Tokyo Chemical Industry Co., Ltd. (Japan), sodium dodecyl sulfate was provided by Merck (Japan). NaOH was provided by Sigma Aldrich (Japan).

Preparation of the organic solution. The initial solution was prepared by dissolving P3HT in THF at a concentration of 5mg/mL. The solution was stirred and heated at 65°C overnight to completely dissolve the polymer. Solution used in this work ranged from 0.1 mg/mL to 1 mg/mL. Polymer solution were used after filtration through a hydrophobic filter (PTFE) of 0.45 µm pore size.

Milli-fluidic setups. Pressure flow controller (FlowEZ 7000), linker (Lineup Link) and flowmeter (Flow Unit) were provided by Fluigent. Pumps and flowmeters could be controlled by PC using the software provided by fluigent (A-I-O). The pressure source for the pressure controllers was a compressor (EARTH MAN ACP-10A) reaching 7 bars and equipped with an air cleaning filter. The syringe pump was provided by kdScientific™ (model KDS-230). Syringe of 5mL were used during those experiments, provided by Terumo®. Microfluidic PEEK tubing (1/16" outside diameter), connectors were purchased from IDEX. Bigger tubing (3mm and 4mm outside diameter) were bought from monotaro (Japan). The temperature of the millifluidic mixers was measured with a heat sensor on top of the chip.
For the first T junction mixer (T Teflon), a Teflon T was drilled through allowing a needle (size: 18 G) to bring the solvent solution in a PTFE tubing. Inner diameters for this co-flow devices are 2 mm and 0.84 mm for water inlet and THF inlet respectively (Figure 1b). The two other millifluidic mixers, T-PEEK and m-CIJ mixers, were fabricated with PEEK - a polymer inert to chemicals and mechanically strong - using a 3D printer. Funmat HT 3D printer provided by Intamsys was used. The PEEK filament was bought from Vision Miner (ThermaX™ PEEK). After printing, devices were annealed at 150°C for 30 minutes, followed by a second annealing at 200°C for 30 minutes and a final annealing at 150°C for 30 minutes. A glass slide was glued with Masterbond® EP29LPSP to the device to allow visualisation and sealing of the channel. After preparing the surface – whipping with acetone and isopropanol – the glue was applied on the glass and put on top of the chip. An annealing at 75°C for 10h was then performed. Finally, tubes were bonded with an UV cured glue. The dimensions of the T PEEK millifluid mixer are as follow: square-shaped water inlet with a section of 2 × 2 mm² and a round-shaped solvent inlet (PEEK tubing) with 1/32" inner diameter (~0.79 mm).

Dynamic light scattering (DLS). Particles size were measured thanks to Nano Particle Analyzer SZ-100V2 provided by Horiba. For each sample, three measurements were done using a quartz cuvette of 1 cm side holding around 3mL of solution using the detector at 90°. Average diameter and polydispersity index (PDI) were determined using cumulants method.

3. Results and discussion

To conduct this study on nanoparticle synthesis by milli-fluidic systems, P3HT was selected as reference since this material has been widely studied and its properties are well-known and established.

P3HT nanoparticles were prepared using nanoprecipitation technique. This method consists in injecting a polymer solution (solvent) into a miscible anti-solvent. By diffusion of the anti-solvent in the solvent, super-saturation of the environment occurs leading to a nucleation and growth of the polymer into nanoparticles. The size of the nanoparticles depends on various parameters such as the concentration of the starting polymer solution, the solvent/anti-solvent ratio,[20] as well as the mixing time.[24] Turbulence affects the mixing time and can be estimated by the Reynolds number. In this work, millifluidic chips are developed to modify the turbulence and understand its influence on the NP size (Figure 1b). The variation of solvent/anti-solvent ratio was given by the difference of flow rate and the diameter difference.

3.1 Optimisation of the concentration

First, the concentration of the solution and the solvent/anti-solvent ratio have to be selected to find a balance between the size of the particles and the final concentration of the dispersion. Since the concentration of the final dispersion has to be relatively high (< 10 mg/mL) to improve the formation of the thin film during the fabrication of the solar cell,[7,34,35] a balance between NP size – which generally increases with increasing concentration – and resulting concentration needed to be found. The influence of the concentration and the solvent/anti-solvent ratio on the NP size was studied with the batch method. Two solvent/anti-solvent ratios, 1/10 and 1/20, and three concentrations, 0.1 mg ml^{-1}, 0.5 mg ml^{-1} and 1 mg ml^{-1}, were studied. The size of the formed nanoparticles decreases with the decreasing concentration, from 159 nm to 109 nm for 1/10 ratio (Table 1), in accordance with the literature.[36] Indeed, when the polymer concentration increased in the solvent, the number of molecules in the solvent droplet increased, leading to more molecules to precipitate and thus a bigger particle. Decreasing the solvent/anti-solvent ratio down to 1/20 lead to further decrease of the NP size, down to 83 nm for 0.1 mg/ml. Since the concentration of 1 mg ml^{-1} was leading to nanoparticles with large diameters, around 135 nm and the 0.1 mg ml^{-1} would lead to a very low final concentration, the intermediate concentration of 0.5 mg ml^{-1} was chosen as the balance between the concentration of the final suspension and the nanoparticles size.

Table 1. Average diameter and PDI measured by DLS (cumulants method) for P3HT nanoparticles synthesized with the batch method and for different initial concentration (0.1, 0.5 and 1 mg ml^{-1}) and solvent/anti-solvent ratio (1/10 and 1/20). Average values and standard deviation calculated on 5 to 11 measurements from 1 to 3 experiments.

Solvent / anti-solvent ratio	Initial concentration (mg ml^{-1})	Average diameter (nm)	Polydispersity index (PDI)	Number of measurements (experiments)
1/10	1	159 ± 10	0.25 ± 0.11	11 (3)
	0.5	108 ± 20	0.20 ± 0.04	11 (3)
	0.1	109 ± 37	0.23 ± 0.12	8 (2)
1/20	1	135 ± 1	0.15 ± 0.02	5 (1)
	0.5	121 ± 2	0.14 ± 0.03	5 (1)
	0.1	83 ± 2	0.35 ± 0.02	5 (1)

3.2 Pressure to flow rate calibration

Once the initial concentration optimized, the synthesis of the NP was performed on the T-junction milli-fluidic system with 2 mm diameter for water inlet and 0.84 mm for THF injection (Figure 1b, T-Teflon). Calibration of the system was first performed and the pressure has been correlated to a flow rate of liquids. To do so, a pressure was applied to the system for a given time period and the amount of liquid was weighted. The volume of THF could be calculated by measuring the difference of weight of the solution before and after evaporation of the THF. For water flow rate, the water flow rate increases linearly with the pressure, up to 850 ml/min for 1500 mbar. The Reynolds numbers (Re) were estimated for every pressure applied to the system and was found to be between 2000 and 10000 in the T-Teflon mixer. At such high Re, the flow regime is in a transition regime between laminar flow to turbulent flow.[37]

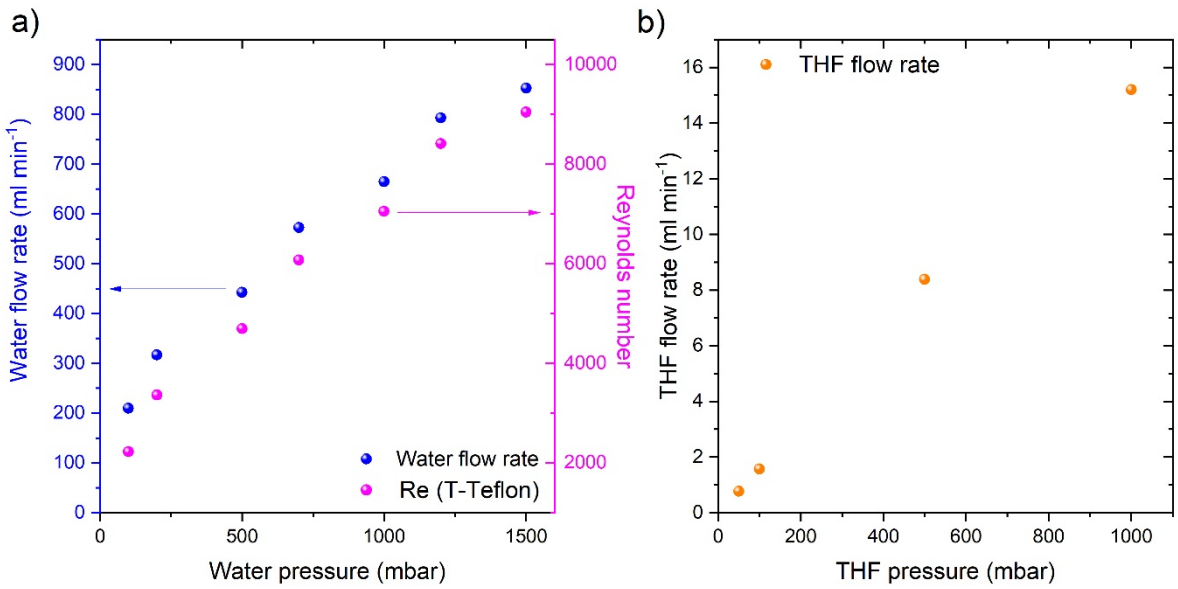

Figure 2. a) Evolution of the water flow rate (left axis) and Reynolds number (right axis) with the pressure for water (anti-solvent) inlet. b) Evolution of the THF flow rate with the THF pressure (solvent) inlet

In the case of the THF flow rate calibration, the flow rate increases linearly with the pressure applied. However, since the channel for water and THF had very different diameter (3mm for water vs 800µm for THF), high flow rates were difficult to achieve with this setup. Only 15 ml min^{-1} could be achieved with a pressure of 1000 mbar.

3.3 Nanoprecipitation in "T" geometry milli-fluidic system

Several parameters can be controlled on the milli-fluidic setup: flow rate of water or THF, temperature of the chip, THF/water ratio. First, the influence of the water flow rate was studied in two kind of co-flow devices: T-Teflon (with a circular section for water and THF inlets of 2 mm and 0.84 mm diameters respectively) and T-PEEK (with a square section of 2 × 2 mm^2 for water inlet and circular THF inlet of 1/32" diameter). The flow rate of THF was set such as to keep a THF/water ratio of 1/100. Figure 3 and Table S1 show the evolution of the NP diameter as a function of the water pressure injected in the chip. Both milli-fluidic chips exhibited the same trend with an average NP diameter decreasing with the increasing water pressure and no significant difference is observed between the two kind of chips. As shown in Figure 2, the pressure is linked to the Reynolds number which is an indicator of the degree of turbulences and chaotic mixing in the chip. The more turbulent the mixing, the smaller the NP. This analysis suggests that the mixing time between the solvent and the anti-solvent could be efficiently decreased by increasing the pressure in the mixer. Consequence is that during the mechanism of NP formation by nanoprecipitation, involving nucleation and then growth, the growth can be stopped prematurely due to increased turbulences in the milli-fluidic chip. However, our systems seem to reach a lower limit for the NP size and starting for 500 mbar, the NP size saturates at around 80 nm. As a result, the smallest NP size achieved was of 83 nm for the T-Teflon at a pressure of 1000 mbars and 78 nm for the T-PEEK at 1000 mbars. The Reynolds numbers was estimated for both devices at 7000. Comparing this millifluidic method with the batch method, with the same initial concentration, the NP diameter decreased from 108 nm to 78 nm when going from a batch method to a milli-fluidic system. This shows that millifluidic mixers can efficiently enhance the turbulences and generate smaller NP size.

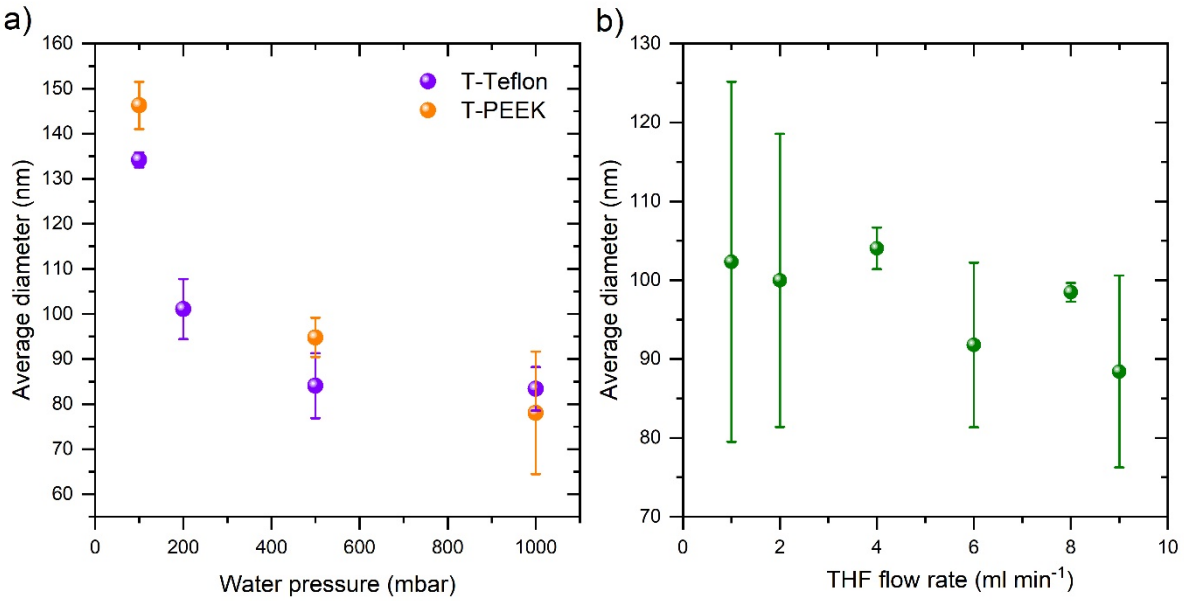

Figure 3. a) Influence of the water flow rate on the average nanoparticle diameters for nanoparticles fabricated with "T" mixer geometry: T-Teflon and T-PEEK. Diameters determined by dynamic light scattering using cumulants method. Average values and standard deviation calculated on 9 to 12 measurements from 3 to 4 experiments. b) Influence of the THF flow rate on the average nanoparticle size (T Teflon, water pressure = 500 mbars). Diameters determined by dynamic light scattering using cumulants method. Average values and standard deviation calculated on 3 to 6 measurements from 1 or 2 experiments.

The influence of the solvent flow rate was also investigated (Figure 3b and Table S2). For this study, the water flow rate was kept constant with a fixed pressure of water (500 mbars). Even though large variation in the NP size were observed, in particular for low THF flow rates, no significant impact could be detected, indicating that the solvent/anti-solvent mixing regime is mainly influenced by the anti-solvent flow rate. Interestingly by changing the solvent flow rate, the ratio solvent/ anti-solvent increased also. However, no change to the diameter of the resulting nanoparticles was observed, indicating that at this low solvent/anti-solvent ratio, this parameter does not influence the size of the particles.

The impact of the temperature of the chip on the NP size has been studied on a T PEEK system. The experiment has been done with the chip at room temperature and heated up at 65°C and for different water pressure (Table S3). Given the variation in size observed in this experiment, no significant differences have been detected between the two experiments, suggesting that the temperature of the chip has little influence on the size of the nanoparticles. Therefore, for simplification of the experiment setup, from now on, all the data gathered are done with the polymer solution stirred at 65°C beforehand and injected in the chip kept at room temperature.

3.4 Nanoprecipitation in "confined impinging jets (CIJ)" geometry milli-fluidic system

In order to reach higher turbulences when the solvent meets the anti-solvent, a different geometry was investigated. This design was inspired by the actual confined inlet jet (CIJ) geometry.[38] Three inlets - two for anti-solvent and one for the solvent - meet into a mixing chamber where nanoprecipitation occurs (Figure 1b, m-CIJ). In this case, pressure was a more relevant parameter than the Reynolds number. Pressure for anti-solvent had to be compensated with solvent pressure. Indeed, when having two wide entries/ one small entry, the pressure applied by the bigger entries creates a large backflow.

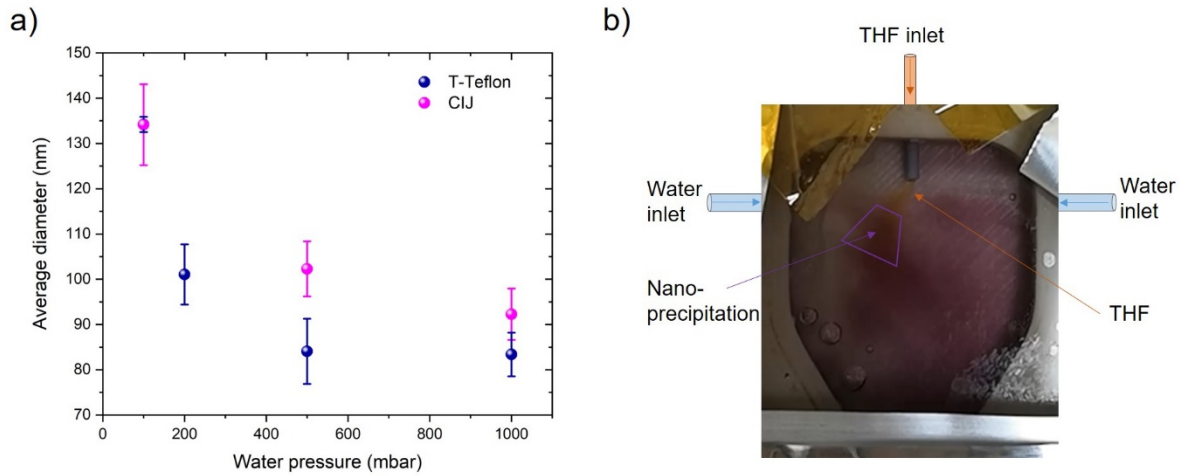

Figure 4: a) Influence of the water pressure in m-CIJ millifluidic chip on the P3HT nanoparticles size. Diameters determined by dynamic light scattering using cumulants method. Average values and standard deviation calculated on 9 measurements from 3 experiments. b) Picture of the nanoprecipitation process in the m-CIJ mixer.

Figure 4 and Table S4 present the impact of the water pressure on the P3HT NP size in m-CIJ chip. Similar to that observed in T geometry, the NP diameter decreases with increasing water pressure in the m-CIJ mixer. The size could be decreased down to 93 nm for 1000 mbar - smaller that the size of NP generated with the batch method. However, the nanoparticles were larger than those obtained in the T geometry chip. The difference in size could be linked to non-homogeneous mixing or dead volume in the mixing chamber and therefore lower turbulences in such kind of mixer.

3.5 Impact of the additives: pH, surfactant and composite donor: acceptor blend

In the first part of this study, we have focused on understanding how the different flow rates of the solvent and anti-solvent can affect the size of the nanoparticles. A plateau in the NP size have been reached at around 80 nm diameter. Additives and pH can also influence the charge environment around the particles and modify the nucleation and growth mechanisms. In particular, charged layers control the interaction of the particles in solution: those charges, when condensing on the surface of the nanoparticles, lead to the repulsion of the nanoparticles, making them less keen to aggregate; if too much charges are condensed, countereffect can happen, leading to the aggregation of the particles.[39,40]

Two strategies were investigated on the T-PEEK chip. First, the impact of the pH of the water (anti-solvent) on the NP size was investigated (Figure 5a and Table S5). When increasing the pH, the number of anions in the solution increases, leading to an accumulation of negative charges around the droplets first and the nanoparticles in a second time.[40,41] When increasing the pH from 7 to 11, the size of the nanoparticles decreased by 20-30 nm for water pressures up to 500 mbar. However, for nanoprecipitation at 1000 mbar of water pressure, no significant influence of being in basic condition is observed on the nanoparticle's sizes. One can suggest that at such high turbulent regime, the nanoparticle size is mainly governed by the rapid mixing time rather than the electrostatic repulsion. For a lower pH of 9, no noticeable changes were observed on the NP size at the different water pressure, suggesting that there is a threshold below which the accumulation of negative charges at the surface of the particles does not impact the size of the NP.

The influence of a surfactant, sodium dodecyl sulfate (SDS) was also investigated (Figure 5b and Table S6). It has been shown that surfactants can influence the size of the NP by nanoprecipitation[6,42] as well as the stability of the colloidal dispersion. At low water pressure, one can see that the surfactant has only a little impact on the size of the NP, with a decrease of around 10 nm of the P3HT NP diameter. At this pressure, the Re is estimated to be ~1500, which is still in the laminar regime. At higher pressure, the Re increase to 4500 or 7500 for 500 and 1000 mbar respectively, and the regime becomes turbulent. In this regime, the addition of SDS seems to have a bigger influence on the size of the NP, decreasing it from 85 nm of diameter down to 62 nm. As shown in the batch method, the addition of surfactant has a important impact on the NP size and this effect seems to be enhanced if the regime is turbulent.

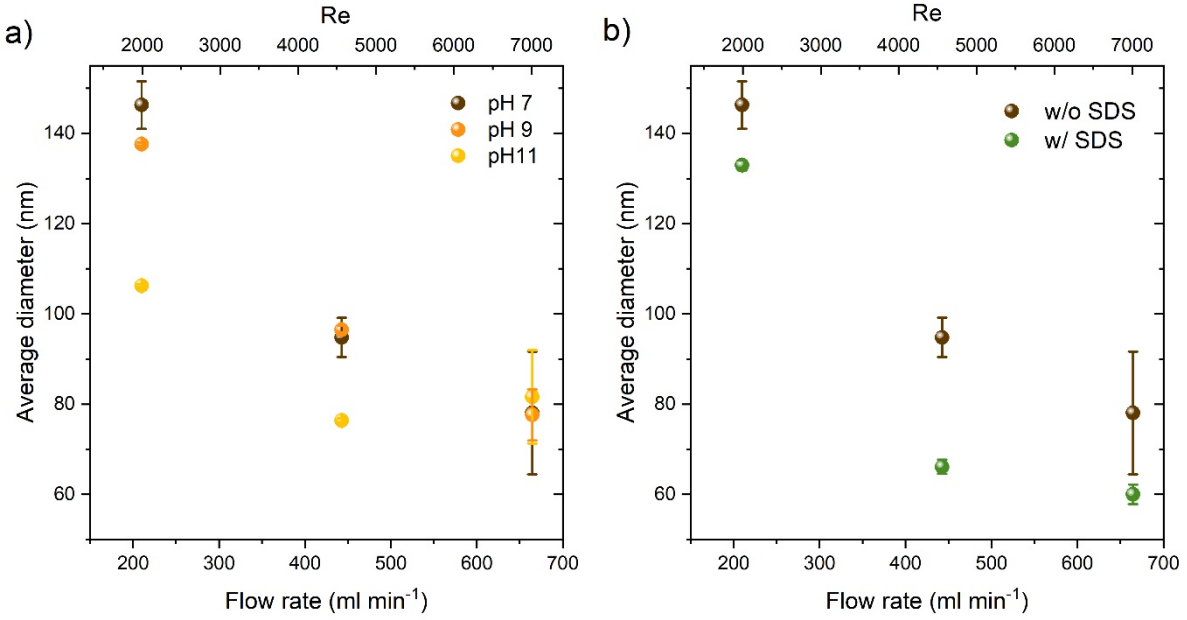

Figure 5. Influence of the pH (a) and the addition of SDS (b) on the size of the nanoparticles generated in "T" geometry millifluidic chips. Diameters determined by dynamic light scattering using cumulants

method. Average values and standard deviation calculated on 3 to 13 measurements from 1 to 5 experiments.

For single component nanoparticles, P3HT in this study, it was not possible to reach diameters below 30 nm with the milli-fluidic systems developed, which would be compatible with the exciton diffusion length. The smallest NP diameter reached was ~ 60 nm (T-PEEK mixer, 1000 mbar, w/ SDS). Therefore, the synthesis of donor:acceptor composite nanoparticles using milli-fluidic system was investigated. In particular, the impact of PCBM on the nanoparticle synthesis was studied. Using the optimized conditions (T-PEEK mixer, water with at 2 mg ml^{-1} SDS as anti-solvent), P3HT:PCBM nanoparticles were synthetized from an initial total concentration in THF of 0.5 mg ml-1 and 1:1 donor:acceptor weight ratio (Table S7). Nanoparticles with average diameters of 49 nm were fabricated, much smaller than those synthesized from pure P3HT solution (~ 60 nm). This preliminary result suggests that the presence of PCBM stabilizes the nuclei during the nanoprecipitation process, leading to smaller particles. Similar effect has already been observed in the case of the synthesis of P3HT NP in DMSO, in which the presence of PCBM showed to increase the zeta potential of the P3HT NP and to generate smaller NP.[43]

As a result, smaller NP were achieved for composite P3HT:PCBM NP, with 49 nm of diameter. Holmes *et al.* showed that nanoprecipitation leads to Janus morphology nanoparticles,[42] therefore one can assume in these nano-objects synthetized by milli-fluidic systems are of the same morphology and that the P3HT and PCBM domain size are compatible with the exciton diffusion length. Further work is ongoing to apply this technique to high efficiency systems such as PTQ10:Y6 and integrate those nano-objects in organic electronic devices in order to understand their potentiality for OPV application.

Conclusion

Nanoprecipitation could be achieved in different kind of milli-fluidic mixers, either with co-flow (refered as “T”) or confined inpinging jets (referred as “m-CIJ”) geometries. By a careful control of different parameters, it was possible to control the size of pure P3HT nanoparticles, from 144 nm down to 60 nm. Mainly, the nanoparticle size could be decrease by increasing the pressure in the milli-fluidic mixer, and thus the turbulences. Similar trends were observed independently of the chip used, either with the two T geometries and the m-CIJ. Turbulence was brought by the pressure of water phase inlet and the decrease of the nanoparticles size by increasing Reynolds number could be demonstrated. However, a plateau was observed for the nanoparticles size which could not be decreased below 80 nm of diameter for P3HT single component NP, a dimension too large compared to the exciton diffusion length. The use of additives in the nanoprecipitation allowed to further decrease the size of P3HT nanoparticles down to 60 nm. Composite donor:acceptor nanoparticles were also synthesized from a P3HT:PCBM solution and the NP size could be further decrease down to 49 nm using the T geometry

mixer with 2 mg ml^{-1} of SDS. This work opens the route for continuous flow synthesis of well-defined organic semiconductors nanoparticles for water-based inks for organic photovoltaics.

Acknowledgments

The authors acknowledge the support provided by the ANR through the WATER-PV project N°ANR-20-CE05-0002 as well as the IRP NextPV, through CNRS (INC and INSIS) and RCAST/University of Tokyo. We also would like to thank Dr. Nicolas Clément and Dr. Simon Grall for the fruitful discussions and help on additive manufacturing.

References

[1] J. Kosco, M. Bidwell, H. Cha, T. Martin, C.T. Howells, M. Sachs, D.H. Anjum, S. Gonzalez Lopez, L. Zou, A. Wadsworth, W. Zhang, L. Zhang, J. Tellam, R. Sougrat, F. Laquai, D.M. DeLongchamp, J.R. Durrant, I. McCulloch, Enhanced photocatalytic hydrogen evolution from organic semiconductor heterojunction nanoparticles, Nat. Mater. 19 (2020) 559–565. https://doi.org/10.1038/s41563-019-0591-1.

[2] N.P. Holmes, S. Chambon, A. Holmes, X. Xu, K. Hirakawa, E. Deniau, C. Lartigau-Dagron, A. Bousquet, Organic semiconductor colloids: From the knowledge acquired in photovoltaics to the generation of solar hydrogen fuel, Curr. Opin. Colloid Interface Sci. 56 (2021) 101511. https://doi.org/10.1016/j.cocis.2021.101511.

[3] H. Piwoński, T. Michinobu, S. Habuchi, Controlling photophysical properties of ultrasmall conjugated polymer nanoparticles through polymer chain packing, Nat. Commun. 8 (2017) 15256. https://doi.org/10.1038/ncomms15256.

[4] H.Y. Liu, P.J. Wu, S.Y. Kuo, C.P. Chen, E.H. Chang, C.Y. Wu, Y.H. Chan, Quinoxaline-based polymer dots with ultrabright red to near-infrared fluorescence for in vivo biological imaging, J. Am. Chem. Soc. 137 (2015) 10420–10429. https://doi.org/10.1021/jacs.5b06710.

[5] A. Holmes, E. Deniau, C. Lartigau-Dagron, A. Bousquet, S. Chambon, N.P. Holmes, Review of Waterborne Organic Semiconductor Colloids for Photovoltaics, ACS Nano. 15 (2021) 3927–3959. https://doi.org/10.1021/acsnano.0c10161.

[6] C. Xie, T. Heumüller, W. Gruber, X. Tang, A. Classen, I. Schuldes, M. Bidwell, A. Späth, R.H. Fink, T. Unruh, I. McCulloch, N. Li, C.J. Brabec, Overcoming efficiency and stability limits in water-processing nanoparticular organic photovoltaics by minimizing microstructure defects, Nat. Commun. 9 (2018) 5335. https://doi.org/10.1038/s41467-018-07807-5.

[7] H. Laval, A. Holmes, M.A. Marcus, B. Watts, G. Bonfante, M. Schmutz, E. Deniau, R. Szymanski, C. Lartigau-Dagron, X. Xu, J.M. Cairney, K. Hirakawa, F. Awai, T. Kubo, G. Wantz, A. Bousquet, N.P. Holmes, S. Chambon, Toward High Efficiency Water Processed Organic Photovoltaics: Controlling the Nanoparticle Morphology with Surface Energies, Adv.

Energy Mater. 13 (2023) 2300249. https://doi.org/10.1002/aenm.202300249.

[8] Y. Tamai, Y. Matsuura, H. Ohkita, H. Benten, S. Ito, One-dimensional singlet exciton diffusion in poly(3-hexylthiophene) crystalline domains, J. Phys. Chem. Lett. 5 (2014) 399–403. https://doi.org/10.1021/jz402299a.

[9] O. V Mikhnenko, P.W.M. Blom, T.-Q. Nguyen, Exciton diffusion in organic semiconductors, Energy Environ. Sci. 8 (2015) 1867–1888. https://doi.org/10.1039/C5EE00925A.

[10] P.E. Shaw, A. Ruseckas, I.D.W. Samuel, Exciton diffusion measurements in poly(3-hexylthiophene), Adv. Mater. 20 (2008) 3516–3520. http://www.scopus.com/inward/record.url?eid=2-s2.0-54949112845&partnerID=40&md5=0ef8c06f2b1ebf4323e9b4247698a285.

[11] L. Zhu, M. Zhang, J. Xu, C. Li, J. Yan, G. Zhou, W. Zhong, T. Hao, J. Song, X. Xue, Z. Zhou, R. Zeng, H. Zhu, C.C. Chen, R.C.I. MacKenzie, Y. Zou, J. Nelson, Y. Zhang, Y. Sun, F. Liu, Single-junction organic solar cells with over 19% efficiency enabled by a refined double-fibril network morphology, Nat. Mater. 21 (2022) 656–663. https://doi.org/10.1038/s41563-022-01244-y.

[12] G. Yu, J. Gao, J.C. Hummelen, F. Wudl, a. J. Heeger, Polymer Photovoltaic Cells: Enhanced Efficiencies via a Network of Internal Donor-Acceptor Heterojunctions, Science (80-.). 270 (1995) 1789–1791. https://doi.org/10.1126/science.270.5243.1789.

[13] T.S. Gehan, M. Bag, L. a Renna, X. Shen, D.D. Algaier, P.M. Lahti, T.P. Russell, D. Venkataraman, Multiscale Active Layer Morphologies for Organic Photovoltaics Through Self-Assembly of Nanospheres., Nano Lett. 14 (2014) 5238–5243. https://doi.org/10.1021/nl502209s.

[14] T. Kietzke, D. Neher, K. Landfester, R. Montenegro, R. Guntner, U. Scherf, Novel approaches to polymer blends based on polymer nanoparticles, Nat Mater. 2 (2003) 408–412. http://dx.doi.org/10.1038/nmat889.

[15] T. Kietzke, D. Neher, M. Kumke, R. Montenegro, K. Landfester, U. Scherf, A Nanoparticle Approach To Control the Phase Separation in Polyfluorene Photovoltaic Devices, Macromolecules. 37 (2004) 4882–4890. https://doi.org/10.1021/ma049625y.

[16] N.P. Holmes, K.B. Burke, P. Sista, M. Barr, H.D. Magurudeniya, M.C. Stefan, a. L.D. Kilcoyne, X. Zhou, P.C. Dastoor, W.J. Belcher, Nano-domain behaviour in P3HT:PCBM nanoparticles, relating material properties to morphological changes, Sol. Energy Mater. Sol. Cells. 117 (2013) 437–445. https://doi.org/10.1016/j.solmat.2013.06.003.

[17] S. Ulum, N. Holmes, D. Darwis, K. Burke, a. L. David Kilcoyne, X. Zhou, W. Belcher, P. Dastoor, Determining the structural motif of P3HT:PCBM nanoparticulate organic photovoltaic devices, Sol. Energy Mater. Sol. Cells. 110 (2013) 43–48. https://doi.org/10.1016/j.solmat.2012.11.015.

[18] S. Ulum, N. Holmes, M. Barr, A.L.D. Kilcoyne, B. Bin Gong, X. Zhou, W. Belcher, P.

Dastoor, The role of miscibility in polymer:fullerene nanoparticulate organic photovoltaic devices, Nano Energy. 2 (2013) 897–905. https://doi.org/10.1016/j.nanoen.2013.03.009.

[19] K. Miladi, S. Sfar, H. Fessi, A. Elaissari, Nanoprecipitation Process: From Particle Preparation to In Vivo Applications, in: C. Vauthier, G. Ponchel (Eds.), Polym. Nanoparticles Nanomedicines, Springer International Publishing, Cham, 2016: pp. 17–53. https://doi.org/10.1007/978-3-319-41421-8_2.

[20] J. Aubry, F. Ganachaud, J.-P. Cohen Addad, B. Cabane, Nanoprecipitation of Polymethylmethacrylate by Solvent Shifting:1. Boundaries, Langmuir. 25 (2009) 1970–1979. https://doi.org/10.1021/la803000e.

[21] S. Gärtner, M. Christmann, S. Sankaran, H. Röhm, E.-M. Prinz, F. Penth, A. Pütz, A.E. Türeli, B. Penth, B. Baumstümmler, A. Colsmann, Eco-Friendly Fabrication of 4% Efficient Organic Solar Cells from Surfactant-Free P3HT:ICBA Nanoparticle Dispersions, Adv. Mater. 26 (2014) 6653–6657. https://doi.org/10.1002/adma.201402360.

[22] A. Holmes, H. Laval, M. Guizzardi, V. Maruzzo, G. Folpini, N. Barbero, E. Deniau, M. Schmutz, S. Blanc, A. Petrozza, G.M. Paternò, G. Wantz, S. Chambon, C. Lartigau-Dagron, A. Bousquet, Water-based solar cells over 10% efficiency: designing soft nanoparticles for improved processability, Energy Environ. Sci. 17 (2024) 1107–1116. https://doi.org/10.1039/D3EE03744D.

[23] C. Xie, X. Tang, M. Berlinghof, S. Langner, S. Chen, A. Späth, N. Li, R.H. Fink, T. Unruh, C.J. Brabec, Robot-Based High-Throughput Engineering of Alcoholic Polymer: Fullerene Nanoparticle Inks for an Eco-Friendly Processing of Organic Solar Cells, ACS Appl. Mater. Interfaces. 10 (2018) 23225–23234. https://doi.org/10.1021/acsami.8b03621.

[24] B. Johnson, R. Prud'homme, Mechanism for Rapid Self-Assembly of Block Copolymer Nanoparticles, Phys. Rev. Lett. 91 (2003) 118302. https://doi.org/10.1103/PhysRevLett.91.118302.

[25] R. Couto, S. Chambon, C. Aymonier, E. Mignard, B. Pavageau, A. Erriguible, S. Marre, Microfluidic supercritical antisolvent continuous processing and direct spray-coating of poly(3-hexylthiophene) nanoparticles for OFET devices, Chem. Commun. 51 (2015) 1008–1011. https://doi.org/10.1039/c4cc07878k.

[26] K. Fischer, P. Marlow, F. Manger, C. Sprau, A. Colsmann, Microfluidics: Continuous-Flow Synthesis of Nanoparticle Dispersions for the Fabrication of Organic Solar Cells, Adv. Mater. Technol. 7 (2022) 2200297. https://doi.org/10.1002/admt.202200297.

[27] B.K. Johnson, R.K. Prud, Chemical Processing and Micromixing in Confined Impinging Jets, 49 (2003).

[28] J. Seaberg, S. Kaabipour, S. Hemmati, J.D. Ramsey, A rapid millifluidic synthesis of tunable polymer-protein nanoparticles, Eur. J. Pharm. Biopharm. 154 (2020) 127–135. https://doi.org/https://doi.org/10.1016/j.ejpb.2020.07.006.

[29] T.-T. Tran, M.-H. Nguyen, Y.Z. Tan, J.W. Chew, S.A. Khan, K. Hadinoto, Millifluidic synthesis of amorphous drug-polysaccharide nanoparticle complex with tunable size intended for supersaturating drug delivery applications, Eur. J. Pharm. Biopharm. 112 (2017) 196–203. https://doi.org/https://doi.org/10.1016/j.ejpb.2016.11.030.

[30] S. Rezvantalab, M. Keshavarz Moraveji, Microfluidic assisted synthesis of PLGA drug delivery systems, RSC Adv. 9 (2019) 2055–2072. https://doi.org/10.1039/C8RA08972H.

[31] J. Ahn, J. Ko, S. Lee, J. Yu, Y. Kim, N.L. Jeon, Microfluidics in nanoparticle drug delivery; From synthesis to pre-clinical screening, Adv. Drug Deliv. Rev. 128 (2018) 29–53. https://doi.org/https://doi.org/10.1016/j.addr.2018.04.001.

[32] E. Lepeltier, C. Bourgaux, P. Couvreur, Nanoprecipitation and the “Ouzo effect”: Application to drug delivery devices, Adv. Drug Deliv. Rev. 71 (2014) 86–97. https://doi.org/https://doi.org/10.1016/j.addr.2013.12.009.

[33] S. Libi, B. Calenic, C.E. Astete, C. Kumar, C.M. Sabliov, Investigation on hemolytic effect of poly(lactic co-glycolic) acid nanoparticles synthesized using continuous flow and batch processes, Nanotechnol. Rev. 6 (2017) 209–220. https://doi.org/10.1515/ntrev-2016-0045.

[34] F.J.M. Colberts, M.M. Wienk, R.A.J. Janssen, Aqueous Nanoparticle Polymer Solar Cells: Effects of Surfactant Concentration and Processing on Device Performance, ACS Appl. Mater. Interfaces. 9 (2017) 13380–13389. https://doi.org/10.1021/acsami.7b00557.

[35] C. Xie, A. Classen, A. Späth, X. Tang, J. Min, M. Meyer, C. Zhang, N. Li, A. Osvet, R.H. Fink, C.J. Brabec, Overcoming Microstructural Limitations in Water Processed Organic Solar Cells by Engineering Customized Nanoparticulate Inks, Adv. Energy Mater. 8 (2018) 1702857. https://doi.org/10.1002/aenm.201702857.

[36] G. Prunet, L. Parrenin, E. Pavlopoulou, G. Pecastaings, C. Brochon, G. Hadziioannou, E. Cloutet, Aqueous PCDTBT:PC $_{71}$ BM Photovoltaic Inks Made by Nanoprecipitation, Macromol. Rapid Commun. 39 (2018) 1700504. https://doi.org/10.1002/marc.201700504.

[37] Y.C. Fung, Biomechanics, Springer New York, New York, NY, 1990. https://doi.org/10.1007/978-1-4419-6856-2.

[38] J. Han, Z. Zhu, H. Qian, A.R. Wohl, C.J. Beaman, T.R. Hoye, C.W. Macosko, A simple confined impingement jets mixer for flash nanoprecipitation, J. Pharm. Sci. 101 (2012) 4018–4023. https://doi.org/10.1002/jps.23259.

[39] A.I. Abdel-Fattah, M.S. El-Genk, Sorption of Hydrophobic, Negatively Charged Microspheres onto a Stagnant Air/Water Interface, J. Colloid Interface Sci. 202 (1998) 417–429. https://doi.org/https://doi.org/10.1006/jcis.1998.5442.

[40] X. Wang, X. Li, S. Yang, Influence of pH and SDBS on the Stability and Thermal Conductivity of Nanofluids, Energy & Fuels. 23 (2009) 2684–2689. https://doi.org/10.1021/ef800865a.

[41] F. Yang, Q. Niu, Q. Lan, D. Sun, Effect of dispersion pH on the formation and stability of

Pickering emulsions stabilized by layered double hydroxides particles, J. Colloid Interface Sci. 306 (2007) 285–295. https://doi.org/https://doi.org/10.1016/j.jcis.2006.10.062.

[42] A. Holmes, H. Laval, M. Schmutz, S. Blanc, J. Allouche, B. Watts, G. Wantz, N.P. Holmes, K. Hirakawa, E. Deniau, S. Chambon, C. Lartigau-Dagron, A. Bousquet, Janus organic semiconductor nanoparticles prepared by simple nanoprecipitation, Mater. Today Chem. 26 (2022) 101229. https://doi.org/10.1016/j.mtchem.2022.101229.

[43] A. Palacio Valera, C. Schatz, E. Ibarboure, T. Kubo, H. Segawa, S. Chambon, Elaboration of PCBM Coated P3HT Nanoparticles: Understanding the Shell Formation, Front. Energy Res. 6 (2019) 1–11. https://doi.org/10.3389/fenrg.2018.00146.